Assessment of nonlocal nuclear potentials in α decay

J. E. Perez Velasquez* and N. G. Kelkar†
Departamento de Fisica, Universidad de los Andes, Cra.1E No.18A-10, Bogotá, Colombia

N. J. Upadhyay‡
School of Physical Sciences, UM-DAE Centre for Excellence in Basic Sciences, Vidyanagari, Mumbai 400098, India

(Received 14 October 2018; revised manuscript received 10 December 2018; published 11 February 2019)

Different models for the nonlocal description of the nuclear interaction are compared through a study of their effects on the half-lives of radioactive nuclei decaying by the emission of alpha particles. The half-lives are evaluated by considering a preformed α particle (^{4}He nucleus), which tunnels through the Coulomb barrier generated by its interaction with the daughter nucleus. An effective potential obtained from a density-dependent double-folding strong potential between the α and the daughter nucleus within the nonlocal framework is found to decrease the half-lives as compared to those in the absence of nonlocalities. Whereas the percentage decrease within the older Perey-Buck and São Paulo models ranges between 20 to 40% for medium to heavy nuclei, a recently proposed effective potential leads to a decrease of only 2 to 4%. In view of these results, we provide a closer examination of the approximations used in deriving the local equivalent potentials and propose that, apart from the scattering data, the α decay half-lives can be used as a complementary tool for constraining the nonlocality models.

DOI: 10.1103/PhysRevC.99.024308

I. INTRODUCTION

It is not often that reexaming an old and well-studied subject reveals new findings. However, one does find examples of experimental as well theoretical investigations, which, either with more refined tools or alternative theoretical approaches, attempt to probe into supposedly established methods to bring new results and solutions. The cosmological lithium problem is a recent example of such a situation where conventional methods overestimated the ^{7}Li abundance, but the introduction of Tsallis statistics within these methods solved the problem [1]. Another recent example is that of pinning down the D-state probability in the deuteron (a topic that has been a classic problem of nuclear physics) using modern precise measurements of the Lamb shift in the muonic deuterium atom [2]. In the context of the present work, we note that the models for the strong nuclear interaction within the nonlocal framework have been studied for decades with the pioneering works in Refs. [3–5]. Perey and Buck [6] studied scattering using the nonlocal framework and introduced a local equivalent potential. These works were followed up by several others which were able to reproduce the scattering data quite well [7,8]. However, reexamining the nonlocality within a novel approach to the same problem, the authors of Refs. [9,10] revealed some interesting features. To list a few, the framework is flexible to use arbitrary nonlocal potentials, is not sensitive to the choice of the nonlocal form factor [10], and the effective potential has a different behavior in coordinate (r) space for $r \to 0$ as compared to the local equivalent potentials in Refs. [6,8].

Another well-established method in nuclear physics is the treatment of α decay as a tunneling problem for the calculation of half-lives of nuclei with a density-dependent double-folding (DF) potential [11–13]. This method is quite successful in reproducing the half-lives of a range of medium and heavy nuclei [14,15]. However, the effects of nonlocality have not been studied within this model. In the present work, starting from the DF potential between the α (^{4}He nucleus) and the daughter, which exist as a preformed cluster inside the decaying parent nucleus, we obtain effective potentials in three different models and study their effects on the alpha decay half-lives. Though the general finding from all models is a decrease in the half-lives due to nonlocality, the percentage decrease using the model proposed in Ref. [9] is significantly smaller than that proposed in Refs. [6,8].

The article is organized as follows. In Sec. II we present the density-dependent double-folding model used to evaluate the potential between the α and the daughter nucleus followed by the formalism for the evaluation of α decay half-lives within a semclassical approach to the tunneling problem. In Sec. III, the concept of nonlocality and the three models used in the present work are briefly introduced. Two of the models [6,8] are found to differ significantly from the model of Ref. [9] at small distances. Section IV explains the reason behind the discrepancies in the behavior of the local equivalent potentials for $r \to 0$. Section V briefly describes the iterative scheme used for the determination of the scattering wave function and a possible extension to the case of decaying states. In Sec. VI, we present the results and discuss them. Finally, in

*je.perez43@uniandes.edu.co
†nkelkar@uniandes.edu.co
‡neelam.upadhyay@cbs.ac.in

Sec. VII we summarize our findings. Since the nonlocality has no particular importance for elastic scattering and is expected to affect cross sections for reaction processes such as stripping and inelastic scattering [16], we propose that the data on the half-lives of radioactive nuclei can be used as a complementary tool in addition to the scattering data that are generally used to restrict the nonlocality models.

II. FORMALISM FOR α DECAY

The objective of the present work is to examine the differences between the existing models to evaluate effective potentials in the nonlocal framework through their effects on the half-lives of radioactive nuclei that decay by α particle emission. To evaluate these effective potentials, we shall use the density-dependent double-folding alpha-nucleus potential [11], which is often used in calculations of α decay [14]. We assume the existence of a preformed α inside the parent and consider the α decay to be a tunneling problem of the α through the Coulomb barrier created by its interaction with the daughter nucleus. Typically, one considers the tunneling of the α through an r-space potential of the form

$$V(r) = V_n(r) + V_C(r) + \frac{\hbar^2 (l + 1/2)^2}{\mu r^2}, \tag{1}$$

where $V_n(r)$ and $V_C(r)$ are the nuclear and Coulomb parts of the α-nucleus (daughter) potential, r the distance between the centers of mass of the daughter nucleus and α, and μ their reduced mass. The last term represents the Langer modified centrifugal barrier [17]. The width of the radioactive nucleus or its half-life which is related to it, is evaluated with a semiclassical Jeffreys-Wentzel-Kramers-Brillouin (JWKB) approach [18]. With the JWKB being valid for one-dimensional problems, the above modification of the centrifugal barrier from $l(l+1) \rightarrow (l+1/2)^2$ is essential to ensure the correct behaviour of the JWKB radial wave function near the origin as well as the validity of the connection formulas used [19].

Since the aim of the present work is to compare the nonlocal effects in different models, we shall restrict here to the simpler situations of alpha decay of spherical nuclei in the s-wave.

A. α nucleus double-folding potential

The input to the double-folding model is a realistic nucleon-nucleon interaction as given in Ref. [20]. The folded nuclear potential is written as

$$V_n(r) = \lambda \int d\mathbf{r}_1\, d\mathbf{r}_2\, \rho_\alpha(\mathbf{r}_1)\, \rho_d(\mathbf{r}_2)\, v(\mathbf{r}_{12} = \mathbf{r} + \mathbf{r}_2 - \mathbf{r}_1,\, E), \tag{2}$$

where ρ_α and ρ_d are the densities of the α and the daughter nucleus in a decay, $|\mathbf{r}_{12}|$ is the distance between a nucleon in the α and a nucleon in the daughter nucleus, and $v(\mathbf{r}_{12}, E)$ is the M3Y nucleon-nucleon (NN) interaction [20] given as

$$v(\mathbf{r}_{12}, E) = 7999 \frac{\exp(-4\,|\mathbf{r}_{12}|)}{4\,|\mathbf{r}_{12}|} - 2134 \frac{\exp(-2.5\,|\mathbf{r}_{12}|)}{2.5\,|\mathbf{r}_{12}|} + J_{00}\,\delta(\mathbf{r}_{12}), \tag{3}$$

with

$$J_{00} = -276\,(1 - 0.005\,E_\alpha/A_\alpha),$$

where the last term is the so-called "knock-on exchange" term and is usually not included in the calculation of nonlocal nuclear potentials [8,9].

The α particle density is given using a standard Gaussian form [20], namely,

$$\rho_\alpha(r) = 0.4229 \exp(-0.7024\, r^2), \tag{4}$$

and the daughter nucleus density is taken to be

$$\rho_d(r) = \frac{\rho_0}{1 + \exp\left(\frac{r-c}{a}\right)}, \tag{5}$$

where ρ_0 is obtained by normalizing $\rho_d(r)$ to the number of nucleons A_d and the constants are given as $c = 1.07\,A_d^{1/3}$ fm and $a = 0.54$ fm [21]. Equation (2) involves a six-dimensional integral. However, the numerical evaluation becomes simpler if one works in momentum space as shown in Ref. [20]. The constant λ appearing in Eq. (2) for the nuclear potential $V_n(r)$ (which is a part of the total potential $V(r)$ in Eq. (1)), is determined by imposing the Bohr-Sommerfeld quantization condition

$$\int_{r_1}^{r_2} k(r)\, dr = (n + 1/2)\,\pi, \tag{6}$$

where $k(r) = \sqrt{\frac{2\mu}{\hbar^2}\,[|V(r) - E|]}$, n is the number of nodes of the quasibound wave function of α-nucleus relative motion and r_1 and r_2 which are solutions of $V(r) = E$, are the classical turning points. This condition is a requisite for the correct use of the JWKB approximation [11]. The number of nodes are re-expressed as $n = (G - l)/2$, where G is a global quantum number obtained from fits to data [22] and l is the orbital angular momentum quantum number. We choose the values of G as 18 for $N < 82$, 20 for $82 < N \leqslant 126$ and 22 for $N > 126$ as recommended in Ref. [22].

The Coulomb potential $V_C(r)$ is obtained by using a similar double folding procedure with the matter densities of the α and the daughter replaced by their respective charge density distributions ρ_α^C and ρ_d^C. Thus,

$$V_C(r) = \int d\mathbf{r}_1\, d\mathbf{r}_2\, \rho_\alpha^C(\mathbf{r}_1)\, \rho_d^C(\mathbf{r}_2)\, \frac{e^2}{|\mathbf{r}_{12}|}. \tag{7}$$

The charge distributions are taken to have a similar form as the matter distributions, except for the fact that they are normalized to the number of protons in the α and the daughter.

B. Semiclassical approach for half-lives

Considering the α decay to be a tunneling problem, the semiclassical expression for the decay width as obtained from different approaches agrees and is given by [11]

$$\Gamma(E) = P_\alpha \frac{\hbar^2}{2\,\mu} \left[\int_{r_1}^{r_2} \frac{dr}{k(r)} \right]^{-1} e^{-2\int_{r_2}^{r_3} k(r)\, dr}, \tag{8}$$

TABLE I. Comparison of the α decay half-lives evaluated using the double-folding model with experiment [23]. The last column lists the cluster preformation probability P_α, given by Eq. (10).

	Q-Value [MeV]	$\tau_{1/2}^{\text{exp}}$ [s]	$\tau_{1/2}^{\text{theory}}$ [s]	P_α
^{254}Fm	7.307	1.2×10^{4}	0.9×10^{4}	0.75
^{212}Po	8.954	2.99×10^{-7}	6.48×10^{-8}	0.22
^{210}Po	5.407	1.2×10^{7}	4.2×10^{5}	0.035[a]
^{180}W	2.515	5.7×10^{25}	1.2×10^{25}	0.21
^{168}Pt	6.989	2×10^{-3}	0.68×10^{-3}	0.34
^{144}Nd	1.903	7.1×10^{22}	5.1×10^{22}	0.72
^{106}Te	4.290	7×10^{-5}	2.4×10^{-5}	0.34

[a]The small value of P_α can be attributed to the magic number of neutrons, $N = 126$, in ^{210}Po (see Fig. 2(c) in Ref. [13] and the corresponding text for a detailed discussion).

where $k(r) = \sqrt{\frac{2\mu}{\hbar^2}\,[|V(r) - E|]}$ and r_1, r_2 and r_3 are the three classical turning points. The energy E is taken to be the same as the Q value for a given α decay. The factor in front of the exponential arises from the normalization of the bound-state wave function in the region between the turning points r_1 and r_2. The α decay half-life of a nucleus is evaluated as

$$\tau_{1/2}^{\text{theory}} = \frac{\hbar \ln 2}{\Gamma}. \tag{9}$$

The factor P_α in Eq. (8) takes into account the probability for the existence of a preformed cluster of the α and the nucleus. This factor, in principle, can be expressed as an overlap between the wave function of the parent nucleus and the decaying-state wave function describing an α cluster coupled to the residual daughter nucleus. However, such a microscopic undertaking is still considered to be a difficult task [14] and the general approach is to determine P_α simply as a ratio

$$P_\alpha = \tau_{1/2}^{\text{theory}}/\tau_{1/2}^{\text{exp}}. \tag{10}$$

We refer the reader to the review article by Ni and Ren [14] (see Sec. 2.5) for a detailed discussion on this subject. In Table I we list the half-lives calculated in the present work (for the cases which will be studied later in the nonlocal framework) within the double-folding model described above. The experimental half-lives [23] and the corresponding values of P_α calculated using Eq. (10) are also listed in Table I. These values are close to some others found in literature (we refer the reader once again to Ref. [14] for the several references listing these values using different models for α decay). As an example, we mention here a microscopic calculation of the α cluster preformation probability and the decay width, presented for ^{212}Po, within a quartetting function approach [24,25]. Considering the interaction of the quartet with the core nucleus ^{208}Pb within the local density approximation, the authors obtained $P_\alpha = 0.367$ and 0.142 [24] using two different models for the core nucleus. In Ref. [25], the calculations were extended to evaluate P_α for several isotopes of Po. It is gratifying to note that the values in Table I for ^{210}Po and ^{212}Po are close to those found by the microscopic calculations in Refs. [24,25].

Finally, we must mention that the objective of the present work is not to evaluate the exact half-lives, but rather compare the effects of nonlocalities in different models. Hence, we shall set $P_\alpha = 1$ when we compare the half-lives calculated within the different models for nonlocality.

III. NONLOCAL NUCLEAR POTENTIALS AND THEIR LOCAL EQUIVALENT FORMS

The general form of the Schrödinger equation in the presence of nonlocality can be written as

$$-\frac{\hbar^2}{2\mu}\nabla^2\Psi(\mathbf{r}) + [V_L(\mathbf{r}) - E]\Psi(\mathbf{r}) = -\int d\mathbf{r}'\, V_{NL}(\mathbf{r}, \mathbf{r}')\Psi(\mathbf{r}'), \tag{11}$$

where V_L can be some isolated local potential and V_{NL} the nonlocal one. The sources of nonlocalities in literature are globally classified into two types: the Feshbach and the Pauli nonlocality [7]. The Feshbach nonlocality is attributed to inelastic intermediate transitions in scattering processes. In other words, the description of an excitation at a point $\mathbf{r}$ in space followed by an intermediate state which propagates and deexcites at some point $\mathbf{r}'$ to get back to the elastic channel is contained in the right-hand side of Eq. (11). Such a coupling gives rise to a coupled channels Schrödinger equation, which can, in principle, be quite difficult to handle.

The Pauli nonlocality is attributed to the exchange effects that require antisymmetrization of the wave function between the projectile and the target. This kind of nonlocality is usually described in literature [6,8,9] in terms of a factorized form of the potential

$$V_{NL}(\mathbf{r}, \mathbf{r}') = U_N\left(\frac{1}{2}|\mathbf{r} + \mathbf{r}'|\right)\frac{\exp\left[-\left(\frac{\mathbf{r}-\mathbf{r}'}{\beta}\right)^2\right]}{\pi^{3/2}\beta^3}, \tag{12}$$

involving a nonlocality range parameter β, which, in the limit $\beta \to 0$ brings us back to the local potential.

In what follows, we shall consider three different approaches to construct the effective potential (U_L) in literature that are based on this kind of description and eventually study the manifestation of the nonlocality in the α decay of some heavy nuclei within these models. Without getting into the complete details of the formalisms, we shall describe the three models briefly along with the behavior of the obtained effective potentials in the subsections below.

A. Perey and Buck model

An energy-independent nonlocal potential U_N for the elastic scattering of neutrons from nuclei was suggested in Ref. [6] to study how far the energy dependence of the phenomenological local potentials that had been used earlier could be accounted for by the nonlocality. The point of view taken was that though part of the energy dependence of the potentials was intrinsic, part of it came from nonlocality. To facilitate the numerical calculation (which involved solving the wave equation in its integrodifferential form to reproduce the experimental data on neutron scattering up to 24 MeV), it was

assumed that $V_{NL}(\mathbf{r}, \mathbf{r}')$ can be factorized as in Eq. (12). Apart from performing numerical calculations and fitting parameters to scattering data that were very well reproduced, the authors provided a method to evaluate the local equivalent (LE) potentials.

Let us review the method and the approximations used to later examine the differences in the effective potentials of Refs. [6,8,9]. Using the factorized form of Eq. (12) the nonlocal Schrödinger equation is given as

$$\left[\frac{\hbar^2}{2\mu}\nabla^2 + E\right]\Psi_N(\mathbf{r}) = \int U_N\left(\frac{1}{2}|\mathbf{r}+\mathbf{r}'|\right)\frac{\exp\left[-\left(\frac{\mathbf{r}-\mathbf{r}'}{\beta}\right)^2\right]}{\pi^{3/2}\beta^3}\Psi_N(\mathbf{r}')\,d\mathbf{r}'. \quad (13)$$

With a change of variables, $\mathbf{r}' - \mathbf{r} = \beta\mathbf{s}$, and using the operator form of the Taylor expansion, the integral on the right-hand side of Eq. (13) can be written as

$$I = \left\{\int \exp\left[\beta\mathbf{s}\cdot\left(\frac{1}{2}\nabla_1 + \nabla_2\right)\right]\frac{\exp[-s^2]}{\pi^{3/2}}\,d\mathbf{s}\right\} \times U_N(\mathbf{r})\,\Psi_N(\mathbf{r}), \quad (14)$$

where ∇_1 operates only on $U_N(\mathbf{r})$ and ∇_2 on $\Psi_N(\mathbf{r})$. Treating the expression $[(1/2)\ \nabla_1 + \nabla_2]$ as an algebraic quantity, the authors evaluated the integral and further neglecting the effect of the operator ∇_1 [i.e., assuming the potential $U_N(r)$ to be approximately constant], the authors obtained the following equation:

$$\left[\frac{\hbar^2}{2\mu}\nabla^2 + E\right]\Psi_N(\mathbf{r}) = U_N \exp[(1/4)\beta^2\nabla^2]\Psi_N(\mathbf{r}) = U_N[\Psi_N(\mathbf{r}) + (1/4)\beta^2\nabla^2\Psi_N(\mathbf{r}) + \cdots]. \quad (15)$$

Considering now the local equation

$$\left[\frac{\hbar^2}{2\mu}\nabla^2 + E\right]\Psi_L(\mathbf{r}) = U_L^{PB}\,\Psi_L(\mathbf{r}) \quad (16)$$

and further assuming, $\Psi_N(\mathbf{r}) \approx \Psi_L(\mathbf{r})$, the authors obtained

$$\nabla^2\Psi_N(\mathbf{r}) = -\frac{2\mu}{\hbar^2}\left(E - U_L^{PB}\right)\Psi_N(\mathbf{r}), \quad (17)$$

which, when substituted in Eq. (15) [and truncating the series in Eq. (15) up to the second term], gives

$$\left[\frac{\hbar^2}{2\mu}\nabla^2 + E\right]\Psi_N(\mathbf{r}) = U_N\Psi_N(\mathbf{r})\left[1 - \frac{1}{4}\beta^2\frac{2\mu}{\hbar^2}\left(E - U_L^{PB}\right)\right] \simeq U_N \exp\left(-\frac{\mu\beta^2}{2\hbar^2}\left(E - U_L^{PB}\right)\right)\Psi_N(\mathbf{r}). \quad (18)$$

Comparing the right-hand sides of Eqs. (16) and (18) [with the assumption $\Psi_N(\mathbf{r}) \approx \Psi_L(\mathbf{r})$], the authors finally obtained

$$U_L^{PB}(r)\exp\left\{\frac{\mu\beta^2}{2\hbar^2}\left[E - U_L^{PB}(r)\right]\right\} = U_N(r). \quad (19)$$

The above equation was, in principle, derived with the assumption that the potential inside the nucleus is constant and the r-dependent form above was justified a posteriori from the results obtained in the paper. Finally, the transcendental equation [Eq. (19)] is solved to obtain $U_L^{PB}(r)$. Taking initially the potentials U_N and U_L^{PB} to be constant to derive the transcendental equation, $U_L^{PB}\exp[\frac{\mu\beta^2}{2\hbar^2}(E - U_L^{PB})] = U_N$, and then introducing the r dependence to get Eq. (19) introduces an inconsistency at small r which will be discussed in Sec. IV.

B. São Paulo potential

Based on conceptually similar considerations as of the Perey and Buck model, a slightly different form of a local equivalent potential was derived in Ref. [8] and applied successfully to reproduce several different scattering data [26–28]. The authors defined the local equivalent potential as

$$U_L^{SP}(r) \approx V_n(r)\exp\left(-\gamma\left[E - V_C(r) - U_L^{SP}(r)\right]\right), \quad (20)$$

where $\gamma = \mu\beta^2/2\hbar^2$ and V_n is the double-folding nuclear potential as described in Sec. II A. The authors cautioned that the local equivalent potential U_L^{SP} is very well described by the above equation except for small distances (i.e., $r \to 0$). Further identifying the factor in the exponential with a velocity

$$v^2 = \frac{2}{\mu}E_k(r) = \frac{2}{\mu}\left[E - V_C(r) - U_L^{SP}(r)\right], \quad (21)$$

the authors mentioned that the effect of the Pauli nonlocality is equivalent to a velocity-dependent nuclear potential. Note that the local equivalent São Paulo potential of Eq. (20) is, in principle, the same as that proposed by Perey and Buck [in Eq. (19)] if we substitute U_N by the double folding potential $V_n(r)$ and neglect the Coulomb potential V_C in Eq. (20).

Both the local equivalent potentials U_L^{SP} and U_L^{PB} are energy dependent and as will be seen later, approach a finite value as $r \to 0$.

C. Mumbai potential

In Ref. [9], the authors proposed a novel method to solve the integrodifferential equation in Eq. (11). The method, which was introduced in Ref. [9], involved the use of the mean value theorem of integral calculus to obtain an effective potential, which, in contrast to the methods discussed so far, was found to be energy independent. Apart from relying on the mathematical validity, the method was further tested by calculating the total and differential cross sections for neutron scattering off ^{12}C, ^{56}Fe, and ^{100}Mo nuclei in the low-energy region (up to 10 MeV) and reasonably good agreement with data was found. We shall refer to this approach of Ref. [9] as the Mumbai approach and briefly review the main steps in their derivation below.

Performing a partial wave expansion of $V_{NL}(\mathbf{r}, \mathbf{r}')$ and $\Psi(\mathbf{r}')$ in Eq. (11), one obtains the radial equation, which, in

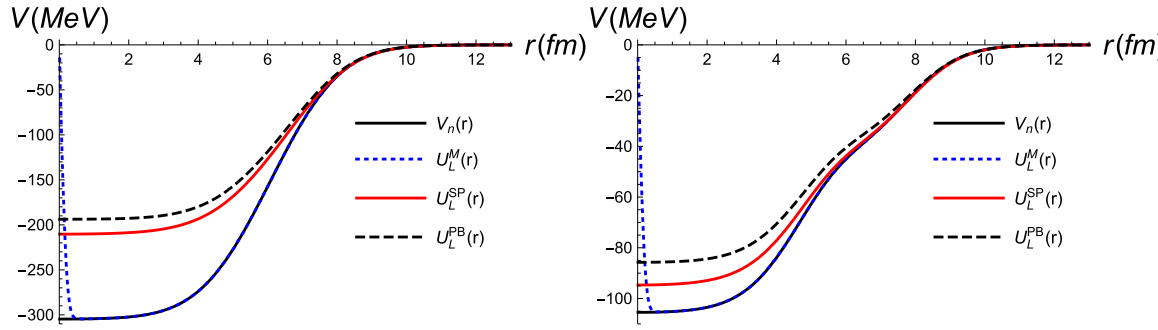

FIG. 1. The strong interaction potential between the alpha (^{4}He) and the daughter nucleus (^{206}Pb) in the decay of ^{210}Po. The left panel shows a comparison of the potentials, $U_L^{SP}(r)$ (dot-dashed line), $U_L^{PB}(r)$ (dashed line), $U_L^M(r)$ (dotted line), and the double folding potential $V_n(r)$ (solid line) with the knock-on exchange term included. The right panel shows the same without the exchange term. For the sake of this comparison, we choose $\lambda = 1$ in Eq. (2).

the absence of the spin-orbit interaction is given as

$$\frac{\hbar^2}{2\mu}\left(\frac{d^2}{dr^2} - \frac{l(l+1)}{r^2}\right)u_l(r) + Eu_l(r) = \int_0^\infty g_l(r,r')u_l(r')\,dr', \tag{22}$$

where

$$g_l(r,r') = \left(\frac{2rr'}{\sqrt{\pi}\beta^3}\right)\exp\left(\frac{-r^2-r'^2}{\beta^2}\right) \times \int_{-1}^{1} U_N\left(\frac{|\mathbf{r}+\mathbf{r}'|}{2}\right)\exp\left(\frac{2rr'x}{\beta^2}\right)P_l(x)\,dx. \tag{23}$$

Making use of the mean value theorem to rewrite the integral on the right-hand side of Eq. (22) and restricting the upper limit of integration to the range of the nuclear interaction, after some algebra, the authors obtained an effective potential given by [9]

$$U_L^M(r) = \int_0^{r_m} g_l(r,r')\,dr', \tag{24}$$

where $g_l(r,r')$ is written as in Eq. (23). Note, however, that the Mumbai (M) potential, in contrast to that of the Perey-Buck (PB) model and the São Paulo (SP) potential, does not depend on energy. Indeed, it also displays a different behavior at small distances with $U_L^M \to 0$ for $r \to 0$.

D. Behavior of U_L in the three models

In Fig. 1, we compare the effective potentials to the double-folding potential $V_n(r)$. To perform this comparison, we choose $\lambda = 1$ in Eq. (2). Thus, replacing $U_N(r)$ with $V_n(r)$ of Eq. (2), the Perey-Buck local equivalent potential $[U_L^{PB}(r)]$ is evaluated using Eq. (19), the São Paulo local equivalent potential $[U_L^{SP}(r)]$ is evaluated using Eq. (20) and the local effective Mumbai potential $[U_L^M(r)]$ using Eq. (24). Since the exchange term in Eq. (3) is often not included in the calculation of the local equivalent potentials [9] (to avoid double counting of the Pauli nonlocality), we show the potentials with (left panel) as well as without (right panel) this term included. The three potentials, $U_L^{PB}(r)$, $U_L^{SP}(r)$, and $U_L^M(r)$ are evaluated for a double-folding potential between an α and ^{206}Pb nucleus, which are the decay products (and hence originally the cluster nuclei) in the α decay of ^{210}Po. The nonlocality parameter β is taken to be 0.22 fm (explanation given in Sec. VI), following the prescription given in Ref. [30]. The São Paulo and Perey-Buck potentials are quite similar, as expected, while the energy-independent Mumbai potential, as mentioned earlier, behaves differently at small r. The latter, as we shall see in the next section with the example of a simple form for U_N, follows quite simply from the nonlocal radial equation. The discrepancy between U_L^{PB}, U_L^{SP}, and U_L^M probably arises due to the assumptions in the derivation of Eq. (19).

IV. MODEL DEPENDENCE AT SMALL DISTANCES

With the aim of understanding the difference in the small r behavior of the effective potentials mentioned in the previous section, we shall now analyze the nonlocal kernel using a simple rectangular well for the nuclear potential and try to obtain analytical expressions. Let us begin by considering the integral on the right-hand side of Eq. (22), namely, $\int_0^\infty g_l(r,r')\,u_l(r,r')\,dr'$. Given the fact that $g_l(r,r')$ is peaked close to $r = r'$ (see, for example, Figs. 1(a) and 5(a) in Ref. [9]), we perform a Taylor expansion of the wave function about $r = r'$ and write the above integral as

$$u(r)\int_0^\infty g_l(r,r')dr' + \int_0^\infty (r'-r)u'(r)g_l(r,r')dr' + \cdots. \tag{25}$$

For the case of a rectangular well of depth -U_0 and range R, i.e., for $U_N(r) = -U_0\Theta(R-r)$ (where Θ is the Heaviside step function) and assuming $l = 0$ for simplicity, we can evaluate the first integral in Eq. (25) analytically. Retaining only the first term in the expansion (25) we can define

$$U_L(r) = \int_0^\infty g_l(r,r')dr', \tag{26}$$

with

$$g_l(r,r') = \frac{2}{\sqrt{\pi}\beta}U_N\left[\frac{1}{2}(r+r')\right]\exp\left[-\frac{(r^2+r'^2)}{\beta^2}\right]\sinh\frac{2rr'}{\beta^2} = -\frac{2}{\sqrt{\pi}\beta}U_0\Theta\left(R-\frac{r+r'}{2}\right)\exp\left[-\frac{(r^2+r'^2)}{\beta^2}\right] \times \sinh\frac{2rr'}{\beta^2}. \tag{27}$$

One can see that $\Theta = 1$ only for $2R - r - r' > 0$, i.e., $2R - r > r'$ and the upper limit of integration in Eq. (26) changes from ∞ to $2R - r$. If $r > 2R$, r' is negative. Hence, to ensure that $r \leqslant 2R$ we write

$$U_L(r) = \frac{-2U_0}{\sqrt{\pi}\beta}\Theta(2R-r)\int_0^{2R-r} dr' \exp\left[-\frac{(r^2+r'^2)}{\beta^2}\right]\sinh\frac{2rr'}{\beta^2}$$
$$= -\frac{U_0}{2}\Theta(2R-r)\left[erf\left(\frac{2(R-r)}{\beta}\right) + 2erf\left(\frac{r}{\beta}\right) - erf\left(\frac{2R}{\beta}\right)\right]. \quad (28)$$

In the limit, $r \to 0$ (for $\beta > 0$) since $erf(0) = 0$, the potential $U_L(r)$ vanishes. When r is finite, we must consider two cases:

$$U_L(r) = -\frac{U_0}{2}\left[erf\left(\frac{2(R-r)}{\beta}\right) + 2erf\left(\frac{r}{\beta}\right) - erf\left(\frac{2R}{\beta}\right)\right] \quad \forall\ r < R \quad (29)$$
$$= -\frac{U_0}{2}\left[-erf\left(\frac{2|R-r|}{\beta}\right) + 2erf\left(\frac{r}{\beta}\right) - erf\left(\frac{2R}{\beta}\right)\right] \quad \forall\ R < r < 2R. \quad (30)$$

If $\beta \to 0$ (i.e., in the absence of nonlocality) since $erf(\infty) = 1$, $U_L(r) = -U_0$ for $r < R$ and 0 for $R < r < 2R$, as expected.

The above derivation on the one hand justifies the behavior of the Mumbai potential at small r, but on the other hand displays an inconsistency between Eqs. (28) and (19). $U_L^{PB}(r)$ in Eq. (19), approaches a finite value as $r \to 0$ (for finite β) as we already noticed in Fig. 1 with a more realistic form of $U_N(r)$. However, $U_L(r)$, as derived above from the radial nonlocal equation, vanishes for $r \to 0$.

Since the starting point for the derivation of the Mumbai potential is indeed the nonlocal radial equation, it seems to be in agreement with the behavior of $U_L(r)$ as in Eq. (28) but not with that in Eq. (19). The inconsistency between Eq. (19) and Eq. (28) probably arises due to the approximations made in the derivation of Eq. (19).

V. ITERATIVE SCHEMES

Models for the nonlocal nuclear interaction are usually tested for their validity by reproducing scattering data. The solution of the radial equation (22) is obtained by implementing an iterative procedure. The starting point of the iterative procedure involves an effective or local equivalent potential which is a solution of the homogeneous equation such as Eq. (16). For example, the iteration scheme can be started with the local equation

$$\frac{\hbar^2}{2M}\left(\frac{d^2}{dr^2} - \frac{l(l+1)}{r^2}\right)u_l^0(r) + [E - U_L(r)]u_l^0(r) = 0, \quad (31)$$

and followed by

$$\frac{\hbar^2}{2M}\left(\frac{d^2}{dr^2} - \frac{l(l+1)}{r^2}\right)u_l^i(r) + [E - U_L(r)]u_l^i(r)$$
$$= \left[\int_0^R g_l(r,r')u_l^{i-1}(r')\,dr' - U_L(r)u_l^{i-1}(r)\right], \quad (32)$$

where the suffix i denotes the ith order approximation to the correct solution. The upper limit R is the radius at which the contribution of the kernel becomes negligible. The iteration is continued until the logarithmic derivative at R obtained from $u_l^i(r)$ agrees up to a certain reasonable precision with the one calculated from $u_l^{i-1}(r)$. Generally one finds that a few iterations [6,9,10] already lead to a good agreement with the data.

The effect of the nonlocal potentials can, in principle, be tested by calculating the half lives of radioactive nuclei. Restricting ourselves to the discussion of α decay, one can follow a similar iteration scheme as above, however, with the difference that $u_l(r)$ will have different boundary conditions. Considering the decaying nucleus as a resonant state (and noting that there are no incident particles), the solution of the radial equation will be a "Gamow function" [29], which vanishes at the origin and behaves as a purely outgoing wave asymptotically. The so-called correct solution obtained from such an iterative scheme could then be used in a quantum mechanical description of the α particle decay rates. Such an analysis of the α decay of several nuclei could serve as a complementary tool for fixing the parameters or assumptions of the nonlocal models. To find out if such a task is worth undertaking, in the present work we take the first step of comparing the α decay half-lives of some heavy nuclei using different models of the local equivalent (or effective) potentials which satisfy the homogeneous equation. The latter allows us to follow the procedures outlined in Sec. II to evaluate the half-life within the JWKB approximation where the wave function is a solution of the homogeneous equation.

VI. RESULTS AND DISCUSSION

To study the effect of nonlocality in α decay, we evaluate the half-lives of some spherical nuclei (with spin-parity, $J^P = 0^+$), decaying in the s-wave. To calculate the half-lives, we use the density-dependent double-folding model introduced in Sec. II A as input for the evaluation of the effective potentials U_L. Note that the nonlocality appears only in the strong part of the potential to which we add the Coulomb and the centrifugal part as given in Sec. II A. Since the half-lives are evaluated within the semiclassical JWKB approximation, the potentials are required to satisfy

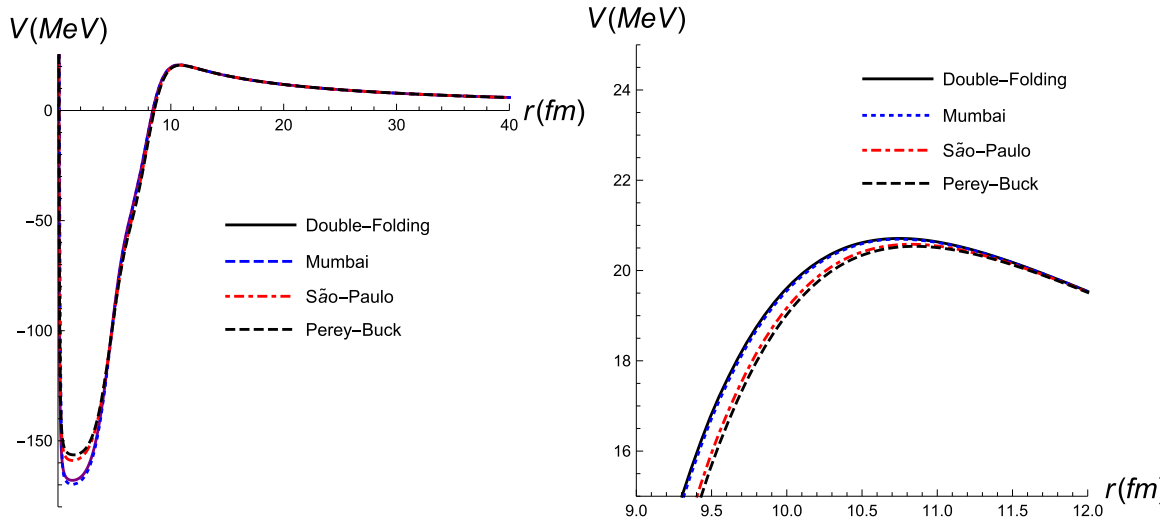

FIG. 2. Comparison of the local equivalent potentials for the interaction between ^{4}He and ^{206}Pb. The full potentials (including the strong and Coulomb interaction as well as the centrifugal part arising due to the Langer term) are displayed in the left panel. The right panel shows the Coulomb barrier on a different scale. The knock-on exchange term is not included. The values of λ appearing in Eq. (2) are listed in Table III.

the Bohr-Sommerfeld condition in Eq. (6) which then fixes the strength of λ in Eq. (2). In Fig. 2, we compare the full potentials (i.e., Eq. (1) for the double folding potential and $U_L(r) + V_C(r) + \frac{\hbar^2 (l+1/2)^2}{\mu r^2}$ for the PB, SP, and M cases) evaluated for the interaction between ^{4}He (α) and ^{206}Pb which form the cluster in ^{210}Po. To evaluate the energy-dependent Perey-Buck and São Paulo potentials, we assume the energy to be the Q-value (which is approximately the kinetic energy of the alpha in the final state) in the decay of ^{210}Po.

Using the three different models for the effective strong interaction, we now evaluate the half-lives in the α decay of medium and heavy nuclei. The nonlocality parameter β is given by $\beta = b_0 m_0/\mu$, where b_0 is the nonlocal range of the nucleon nucleus interaction, m_0 is the nucleon mass, and μ the α-nucleus reduced mass (see Ref. [30] for details). We choose $b_0 = 0.85$ fm as in Ref. [6], so that $\beta = 0.22$ fm. The half-lives evaluated with the nonlocality included are found to decrease as compared to those evaluated using the double-folding model without nonlocality.

The percentage decrease in half-life due to nonlocality is defined as

$$PD = \frac{\tau_{1/2}^{DF} - \tau_{1/2}^{NL}}{\tau_{1/2}^{DF}} \times 100, \tag{33}$$

where, $\tau_{1/2}^{DF}$ is the half-life evaluated in the double folding model without the inclusion of nonlocalities and $\tau_{1/2}^{NL}$ is the one evaluated using the different nonlocal frameworks. We remind the reader that we choose the cluster preformation factor $P_\alpha = 1$ for this comparison.

In Table II we list the percentage decrease in the half-lives of several nuclei. The numbers outside parentheses correspond to calculations with the so-called knock-on exchange term excluded to avoid double counting of the Pauli nonlocality. Inclusion of this term (numbers in parentheses) causes a larger percentage decrease of half-lives due to nonlocality within the Perey-Buck and São Paulo models. The effect of nonlocality is, in general, small within the Mumbai approach. Apart from this, we note that the effect of nonlocality is smaller in the decay of ^{212}Po ($Q = 8.954$ MeV) as compared to ^{210}Po (5.407 MeV). Though the difference is not large, it hints towards a decrease in the effect of nonlocality with increasing energy in the two isotopes.

To understand the results in Table II, let us examine Fig. 2 and the factors presented in Table III. We consider the numbers outside the parentheses in Table II, which means that the knock-on exchange term is not included in the calculation of V_n. The full potentials given in Fig. 2 are obtained using Eqs. (1) and (2) with the values of λ (listed in Table III) being fixed by the Bohr-Sommerfeld condition (6). Assuming $P_\alpha = 1$ and rewriting the expression for the width in Eq. (8) as

$$\Gamma = \frac{\hbar^2}{2\,\mu} NP,$$

where the normalization factor $N = [\int_{r_1}^{r_2} dr/k(r)]^{-1}$ and the exponential factor or the penetration probability $P = e^{-2\int_{r_2}^{r_3} k(r)\,dr}$ we note from Table III that it is indeed the

TABLE II. Percentage decrease, PD as in Eq. (33), in α decay half-lives of nuclei using three different models of nonlocality. Numbers within parentheses include the effect of the so-called knock-on exchange term and those outside ignore this term. The nonlocality parameter $\beta = 0.22$ fm.

	Mumbai	São Paulo	Perey-Buck
^{254}Fm	2.49 (3.85)	31.7 (69.8)	40.3 (71.5)
^{210}Po	3.4 (2.4)	29.9 (66.2)	37.3 (67.9)
^{212}Po	3.26 (3.28)	26.7 (62.0)	33.0 (63.8)
^{180}W	3.8 (4.0)	30.1 (66.1)	37.6 (67.7)
^{168}Pt	4.9 (4.1)	27.5 (62.7)	34.9 (64.9)
^{144}Nd	3.9 (3.8)	25.9 (60.3)	31.2 (61.9)
^{106}Te	3.2 (4.1)	19.4 (51.9)	24.1 (53.6)

TABLE III. Factors contributing to the calculated half-lives in different models. The strength of the strong interaction λ, which is fixed by the Bohr-Sommerfeld condition (6), the normalization factor $N = [\int_{r_1}^{r_2} dr/k(r)]^{-1}$, and the penetration probability $P = e^{-2\int_{r_2}^{r_3} k(r)dr}$, are listed in all models for each of the nuclei considered. The knock-on exchange term is not included.

Isotope	Q-Value [MeV]	Double folding			Mumbai			São Paulo			Perey-Buck		
		λ	P	N [fm^{-2}]	λ	P	N [fm^{-2}]	λ	P	N [fm^{-2}]	λ	P	N [fm^{-2}]
^{254}Fm	7.307	1.95	3×10^{-25}	0.34	1.96	3.1×10^{-25}	0.34	2.08	4.5×10^{-25}	0.34	2.30	5.2×10^{-25}	0.34
^{212}Po	8.954	2.02	3×10^{-14}	0.34	2.03	3.2×10^{-14}	0.34	2.17	4.2×10^{-14}	0.33	2.36	4.6×10^{-14}	0.33
^{210}Po	5.407	2.10	5.4×10^{-27}	0.36	2.12	5.6×10^{-27}	0.35	2.25	7.8×10^{-27}	0.35	2.45	8.6×10^{-27}	0.36
^{180}W	2.515	2.04	2×10^{-46}	0.36	2.05	2.1×10^{-46}	0.36	2.17	2.8×10^{-46}	0.36	2.35	3.1×10^{-46}	0.35
^{168}Pt	6.989	2.08	3×10^{-18}	0.35	2.10	3.2×10^{-18}	0.35	2.22	4.2×10^{-18}	0.35	2.41	4.6×10^{-18}	0.35
^{144}Nd	1.903	2.23	3.6×10^{-44}	0.37	2.26	3.8×10^{-44}	0.37	2.39	4.9×10^{-44}	0.36	2.55	5.3×10^{-44}	0.36
^{106}Te	4.290	2.28	6.2×10^{-17}	0.35	2.30	6.5×10^{-17}	0.35	2.43	7.9×10^{-17}	0.35	2.58	8.4×10^{-17}	0.35

difference in the penetration probabilities P, which leads to the differences in the percentage decrease in the half-lives in Table II. The normalization factors are almost constant in all models. This fact is also reflected in Fig. 2. In the right panel we notice that the Coulomb potential in the São Paulo and Perey-Buck models is shifted to the right as compared to the double-folding and Mumbai potentials. This shift leads to a shift of the second turning point r_2, to bigger values and hence smaller half-lives (due to the bigger exponential factor as can be seen in Table III).

Before closing the discussions, some comments about one of the earliest investigations of nonlocalities in α decay are in order here. In a series of works [31–34], M. L. Chaudhury studied the effects of nonlocalities in α decay of different nuclei. Using an integrodifferential equation similar to that of Frahn and Lemmer [35], in Ref. [31], the author calculated the transmission coefficient (or penetration factor) for α tunneling within the WKB approximation. The point-like Coulomb field was superimposed by a nonlocal α-nucleus interaction based on the Igo potential [36] and a Gaussian form was used for the nonlocal function with a nonlocality parameter of $\beta = 0.9$ fm. Investigating for the α decay of ^{254}Fm in Ref. [31], the penetration factor was found to increase by a factor of 1.7 due to nonlocality. This amounts to a decrease of about 40% in the half-life. The investigation in Ref. [31] was extended to several even-even nuclei and the author once again found a large increase (∼50%) [32] in the penetration factors due to nonlocality. The author further studied the effects of nonlocality in deformed and rare-earth nuclei [33,34] with the inclusion of an exchange term in the nonlocal kernel. Though the calculation in Ref. [31] involves a different nonlocal framework as compared to the models considered in the present work, the 40% decrease in the value of the half-life of ^{254}Fm [31] (evaluated without the exchange term in the nonlocal kernel), is similar to the Perey-Buck model result in Table II, without the inclusion of the knock-on exchange term.

VII. SUMMARY

Investigation of the effects of nonlocality in the nuclear interaction began several decades ago, but has remained to be a topic of continued interest until now. The vast majority of works proposing different approaches to understand the origin as well as the manifestations of the nonlocality concentrate on the reproduction of scattering data. Here we propose the study of the effects of nonlocality on α decay half-lives of nuclei as a complementary tool for determining the nonlocal interaction within different models.

To be specific, we study these effects using three different models available in literature. Though all the three models agree qualitatively on the result that the nonlocal nuclear interaction leads to a decrease in half-lives, the percentage decrease in the three models is quite different. The recent Mumbai model [9,10] predicts a very small percentage decrease of about 2 to 5% in most heavy nuclei studied, however, the Perey-Buck and São Paulo models predict a much bigger decrease of around 20 to 40% (in the absence of the knock-on exchange term).

To understand the above differences, we examined the model assumptions in detail and found an inconsistency in the behavior of the local equivalent potentials, $U_L(r)$, derived by starting with the three-dimensional Schrödinger equation and its radial part. Whereas the former leads to $U_L(r)$ which is finite at the origin, the latter leads to $U_L(r)$ which vanishes as $r \to 0$. Indeed the Perey-Buck and the São Paulo models are of the first type (with the local equivalent potential being finite at $r = 0$), but the effective potential of the Mumbai group vanishes at $r = 0$. Introducing the nonlocal framework to find the Gamow functions corresponding to the decaying nuclei and performing a more exact quantum mechanical calculation of the half-lives to compare with data could possibly provide a better explanation of the different behaviors of the potentials.

ACKNOWLEDGMENTS

The authors are thankful to B. K. Jain for many useful discussions. J.E.P.V. thanks the Faculty of Science, Universidad de los Andes, Colombia, for financial support through Grant No. INV-2017-26-1137. N.G.K. thanks the Faculty of Science, Universidad de los Andes, Colombia for financial support through Grant No. P18.160322.001-17. N.J.U. acknowledges financial support from SERB, Government of India (Grant No. YSS/2015/000900).

[1] S. Q. Hou *et al.*, Astrophys. J. **834**, 165 (2017).
[2] N. G. Kelkar and D. Bedoya Fierro, Phys. Lett. B **772**, 159 (2017).
[3] H. Bethe, Phys. Rev. **103**, 1353 (1956).
[4] W. E. Frahn, Nuovo Cimento **4**, 313 (1956).
[5] R. Peierls and N. Vinh Mau, Nucl. Phys. A **343**, 1 (1980).
[6] F. Perey and B. Buck, Nucl. Phys. **32**, 353 (1962).
[7] A. B. Balantekin, J. F. Beacom, and M. A. Cândido Ribeiro, J. Phys. G **24**, 2087 (1998).
[8] L. C. Chamon *et al.*, Brazilian J. Phys. **33**, 238 (2003).
[9] N. J. Upadhyay, A. Bhagwat, and B. K. Jain, J. Phys. G **45**, 015106 (2018).
[10] N. J. Upadhyay and A. Bhagwat, Phys. Rev. C **98**, 024605 (2018).
[11] N. G. Kelkar and H. M. Castañeda, Phys. Rev. C **76**, 064605 (2007).
[12] N. G. Kelkar, H. M. Castañeda, and M. Nowakowski, Eur. Phys. Lett. **85**, 20006 (2009).
[13] N. G. Kelkar and M. Nowakowski, J. Phys. G **43**, 105102 (2016).
[14] D. Ni and Z. Ren, Ann. Phys. **358**, 108 (2015).
[15] C. Xu and Z. Ren, Nucl. Phys. A **760**, 303 (2005); Phys. Rev. C **74**, 014304 (2006); Nucl. Phys. A **753**, 174 (2005); Phys. Rev. C **73**, 041301(R) (2006).
[16] N. K. Glendenning, *Direct Nuclear Reactions* (Academic, New York, 1983), p. 42.
[17] R. E. Langer, Phys. Rev. **51**, 669 (1937).
[18] N. Fröman, *JWKB Approximation: Contributions to the Theory* (North-Holland, Amsterdam, 1965); N. Fröman and Per Olof Fröman, *Physical Problems Solved by the Phase-Integral Method* (Cambridge University Press, Cambridge, England, 2002).
[19] J. J. Morehead, J. Math. Phys. **36**, 5431 (1995).
[20] G. R. Satchler and W. G. Love, Phys. Rep. **55**, 183 (1979); A. M. Kobos, G. R. Satchler, and A. Budzanowski, Nucl. Phys. A **384**, 65 (1982).
[21] J. D. Walecka, *Theoretical Nuclear Physics and Subnuclear Physics* (Oxford University Press, Oxford, 1995), p. 11; B. Hahn, D. G. Ravenhall, and R. Hofstadter, Phys. Rev. **101**, 1131 (1956).
[22] B. Buck, A. C. Merchant, and S. M. Perez, Phys. Rev. C **45**, 2247 (1992); B. Buck, J. C. Johnston, A. C. Merchant, and S. M. Perez, *ibid.* **53**, 2841 (1996).
[23] J. K. Tuli, *Nuclear Wallet Cards*, NNDC, Brookhaven National Laboratories (2011) (can be downloaded at www.nndc.bnl.gov/wallet).
[24] C. Xu, Z. Ren, G. Röpke, P. Schuck, Y. Funaki, H. Horiuchi, A. Tohsaki, T. Yamada, and B. Zhou, Phys. Rev. C **93**, 011306(R) (2016).
[25] C. Xu, G. Röpke, P. Schuck, Z. Ren, Y. Funaki, H. Horiuchi, A. Tohsaki, T. Yamada, and B. Zhou, Phys. Rev. C **95**, 061306(R) (2017).
[26] L. C. Chamon, D. Pereira, M. S. Hussein, M. A. Cândido Ribeiro, and D. Galetti, Phys. Rev. Lett. **79**, 5218 (1997).
[27] L. C. Chamon, B. V. Carlson, and L. R. Gasques, Phys. Rev. C. **83**, 034617 (2011).
[28] L. C. Chamon, L. R. Gasques, and B. V. Carlson, Phys. Rev. C **84**, 044607 (2011).
[29] A. Mondragon and E. Hernandez, Ann. Physik Leipzig **48**, 503 (1991).
[30] D. F. Jackson and R. C. Johnson, Phys. Lett. B **49**, 249 (1974).
[31] M. L. Chaudhury, Phys. Rev. Lett. **5**, 205 (1960).
[32] M. L. Chaudhury, Phys. Rev. **130**, 2339 (1963).
[33] M. L. Chaudhury, J. Phys. A **4**, 328 (1971).
[34] M. L. Chaudhury and D. K. Sen, J. Phys. **42**, 19 (1981).
[35] W. E. Frahn and R. H. Lemmer, Il Nuovo Cimento **5**, 1564 (1957).
[36] I. Igo and R. M. Thaler, Phys. Rev. **106**, 126 (1957).